NGU REPORT 2024.025

Geophysical Investigation of Traces from Post-Glacial Seismic Activity Using GPR in Brumunddal, Central Norway

GEOLOGY FOR SOCIETY

SINCE 1858

GEOLOGICAL SURVEY OF NORWAY

- NGU -

NGU REPORT 2024.025

Geophysical Investigation of Traces from Post-Glacial Seismic Activity Using GPR in Brumunddal, Central Norway

GEOLOGICAL SURVEY OF NORWAY
- NGU -

NGU REPORT
Geology for society

Geological Survey of Norway
P.O. Box 6315 Torgarden
NO-7491 Trondheim, Norway
Tel. +47 73 90 40 00

Report no.: 2024.025
ISSN: 0800-3416 (print)
ISSN:2387-3515 (digital)
Grading: Open

Title: Geophysical Investigation of Traces from Post-Glacial Seismic Activity Using GPR in Brumunddal, Central Norway
Authors: Georgios Tassis, Inger-Lise Solberg, Ola Fredin
Client: NGU
County: Innlandet
Municipality: Ringsaker

Map-sheet name (M=1:250.000): Hamar
Map-sheet name (M=1:50.000): 1916 I
Deposit name and grid-reference: 289000/6765000 (UTM zone 33 N)
Numbers of pages: 26
Price (NOK): 148,-

Map enclosures: None
Fieldwork carried out: 9-11.06.2020
Date of report: 16.10.2024
Project no.: 381500
Person responsible: Marco Brönner
Keywords: Georadar, GPR, Landslide, Post-Glacial Seismicity, Till

Summary:
This study employed Ground Penetrating Radar (GPR) to investigate subsurface geological features in the Brumunddal area, central Norway, focusing on regions affected by post-glacial seismicity and landslides. Using a central frequency of 100 MHz provided a balance between penetration depth and resolution, enabling mapping of subsurface features located in up to 22.5 meters depth in Hestbekken, Åsdal, and Mælumsætra NE, and up to 27.5 meters in Putten and Skreppåsen. The results revealed variable geological conditions, with some profiles exhibiting more favourable electromagnetic properties in landslide deposits, indicated by stronger and more continuous reflections. However, this correlation was not always consistent. Furthermore, profiles in Hestbekken, showed both weak and strong reflectivity beneath bog, reflecting different water saturation levels. While Åsdal profiles correlated strong reflectivity within landslide materials, Mælumsætra NE showed both distinct and weak reflectors. Additionally, the investigations in Putten and Skreppåsen highlighted the influence of surface conditions on the GPR measurements, and indications of potential faulting in profile S1. Overall, the findings emphasize the importance of considering local geological factors in interpreting GPR data, with potential for further insights through ground truth methods like drilling.

CONTENTS

1. INTRODUCTION 5
2. METHOD DESCRIPTION 5
3. DATA ACQUISITION & PROCESSING 6
4. RESULTS AND INTERPRETATIONS 9
4.1 Hestbekken 9
4.2 Mælumsætra – Åsdal 14
4.3 Mælumsætra NE 18
4.4 Putten and Skreppåsen 21
5. CONCLUSIONS 25
6. References 25

PREFACE

In recent years large areas of Scandinavia including Norway have been scanned using airborne Light Detection and Ranging (LiDAR) techniques that allows for detailed mapping of landforms. Based on this mapping, regions in central southern Norway and Scandinavia show evidence of significant paleoseismic activity leading to widespread occurrences of landslides.

Brumunddal in Central-Southern Norway is one of these areas. As a part of the investigations of these remnants of landslides we decided to use Ground Penetrating Radar (GPR) to map the structures in the sediments below the landslide scars and in the landslide deposits.

The results from the study in Brumunddal will be published in a paper (Fredin, Solberg, Keiding, & Tassis, in prep.), but the paper will only document some of the GPR results. In the present report all the profiles from the GPR investigations are presented and interpreted.

1. INTRODUCTION

The Ground Penetrating Radar (GPR) surveys reported here were conducted as part of a broader project aimed at mapping and studying results of post-glacial seismic activity in central southern Norway. Mapping by use of airborne Light Detection and Ranging (LiDAR) data has revealed traces of numerous landslides in moraine terrain in central Hedmark, northeast of lake Mjøsa (Fredin, Solberg, Keiding, & Tassis, in prep.). Some landforms resemble liquefaction features and sand volcanoes (Olsen, Bergstrøm, Sveian, & Riiber, 2018).

This concentration of landslide scars in a relatively flat terrain strongly suggests that they were triggered by seismic activity after the last deglaciation. To investigate the landforms, and structures in the sediments below the landslide scars and in the landslide deposits it was decided to use GPR. The surveys were conducted at key locations across a wide area northeast of Brumunddal in Ringsaker municipality, an area characterised by generally significant glacial till cover, and landforms of subglacial origin such as drumlins and Rogen moraine.

Fieldwork took place in June 2020, using the Malå RTA (Snake) system, ideal for navigating forested areas where the majority of the profiles were located. The survey employed 100 MHz antennas, which provided a balance between resolution and depth penetration appropriate for the dimensions of the surveyed landforms. Although till can have unpredictable responses to electromagnetic waves, previous GPR applications in other till-rich areas in Norway have yielded valuable insights, suggesting the potential for successful results in this study area as well (Helle, 2004; Lecomte, Thollet, Juliussen, & Hamran, 2008; Burki, Larsen, Fredin, & Margreth, 2009). This study may improve understanding of possible past seismic events and contribute to the investigation of current earthquake risks in central Norway.

2. METHOD DESCRIPTION

Ground Penetrating Radar (GPR), also referred to as Georadar, is an electromagnetic geophysical technique designed to investigate subsurface stratification. It works by transmitting electromagnetic waves into the ground, which then interact with the materials they encounter. These waves propagate through lossy dielectric materials, meaning materials that exhibit energy loss due to absorption and scattering, and they detect changes in material properties or structures (Davis & Annan, 1986).

The transmitted electromagnetic waves move through the subsurface as essentially nondispersive waves, maintaining their shape without significant spreading over distance. When the waves encounter changes in material impedance – such as differences in composition, density, or moisture – they are reflected or scattered. These reflections produce signals that resemble the initial transmitted wave (Butler, 2005). These reflected signals are received at the surface, where they are recorded and processed to reconstruct underground interfaces and structures.

This is accomplished by positioning a series of 1D electromagnetic "soundings" side by side to generate a continuous 2D image, commonly referred to as a radargram (Figure 2.1). The radargram visualizes the subsurface layers, structures, or objects by displaying reflected wave events, enabling geophysicists to interpret material changes and subsurface features.

In lossy dielectric materials, the penetration of electromagnetic waves is limited due to energy absorption, which results in penetration depth becoming a variable that depends on several factors. One of the key determinants is the frequency of the electromagnetic waves used in the GPR system. GPR operates within a frequency range of 1 to 1000 MHz, and the choice of frequency has a direct impact on both the depth of exploration and the resolution of the subsurface features being imaged.

At lower frequencies, the pulses can penetrate deeper into the ground, but the signals tend to disperse more, leading to lower resolution. Conversely, at higher frequencies, the resolution of the signal is improved, allowing for finer details in the resulting radargram. However, the drawback of

using higher frequencies is that the signal absorption by the material becomes stronger, reducing the depth of penetration significantly.

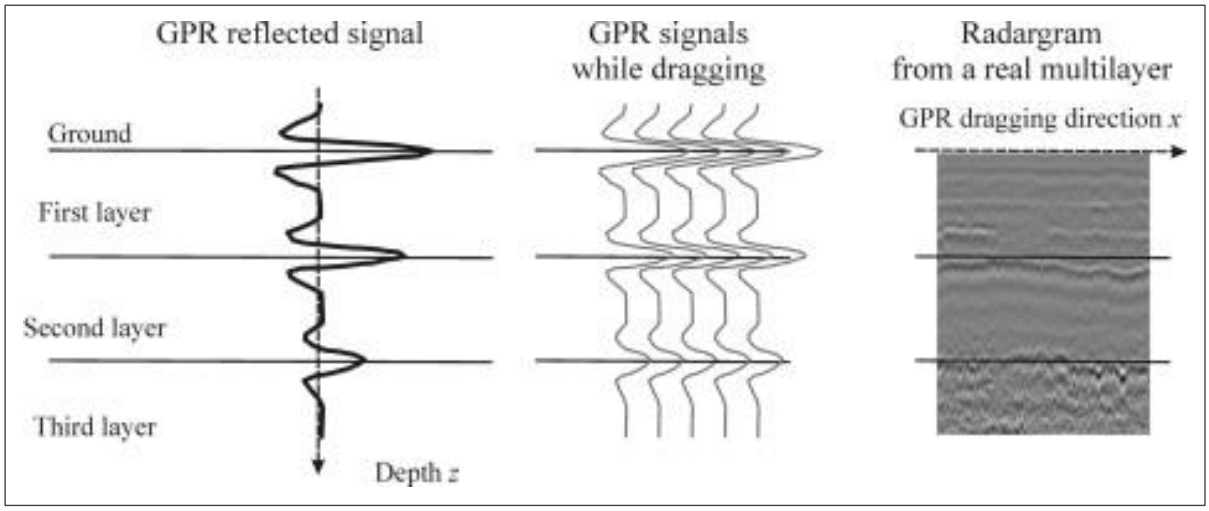

Figure 2.1: From a single GPR trace to a full radargram (Benedetto & Benedetto, 2014).

Therefore, when planning GPR studies, a balance between penetration depth and signal resolution must be achieved by selecting an appropriate frequency based on the goals of the survey. Lower frequencies are selected for deeper exploration, whereas higher frequencies are chosen when higher resolution is needed for imaging shallower subsurface structures. This compromise is essential to maximize the effectiveness of GPR in various geological or environmental conditions.

3. DATA ACQUISITION & PROCESSING

A total of ten GPR profiles were measured across five different locales northeast of Brumunddal, spanning approximately 3.6 kilometers in total. The Malå RTA (Snake) system by Guideline GEO was utilized for this survey. As seen in Figure 3.1, the Snake system uses a parallel endfire configuration where the transmitter and receiver antennas are placed in a row at 2.2 meters from each other. This configuration provides better maneuverability in forested or challenging terrain but results in slightly reduced signal quality compared to the more conventional perpendicular broadside configuration, where antennas are parallel and dragged perpendicularly. However, in field conditions where terrain restrictions make the perpendicular setup impractical, the parallel endfire configuration offers a viable alternative, especially since the degradation in signal quality does not significantly affect the interpretation of the geology (Tassis & Rønning, 2015).

In this survey, a central frequency of 100 MHz was chosen to optimize both resolution and depth penetration, with traces collected at 25-centimeter intervals to achieve detailed imaging of subsurface features throughout the survey area. The maximum time window was set to 750 nanoseconds due to uncertainties about ground permittivity, yielding an estimated depth coverage of about 37.5 meters, assuming a standard wave velocity of 0.1 m/ns.

To control data acquisition, a hip-chain device was used. This method relies on an unrolling thread roll to trigger measurements at consistent intervals, regardless of the operator's walking speed. Positioning along the survey lines was captured with a Garmin GPSMAP 60Cx handheld GPS, which was later corrected for the standard discrepancy with the GPR trace positions (see Figure 3.1). The refined GPS data was then synchronized with the GPR traces, ensuring accurate spatial correlation between the measured GPR data and the survey area.

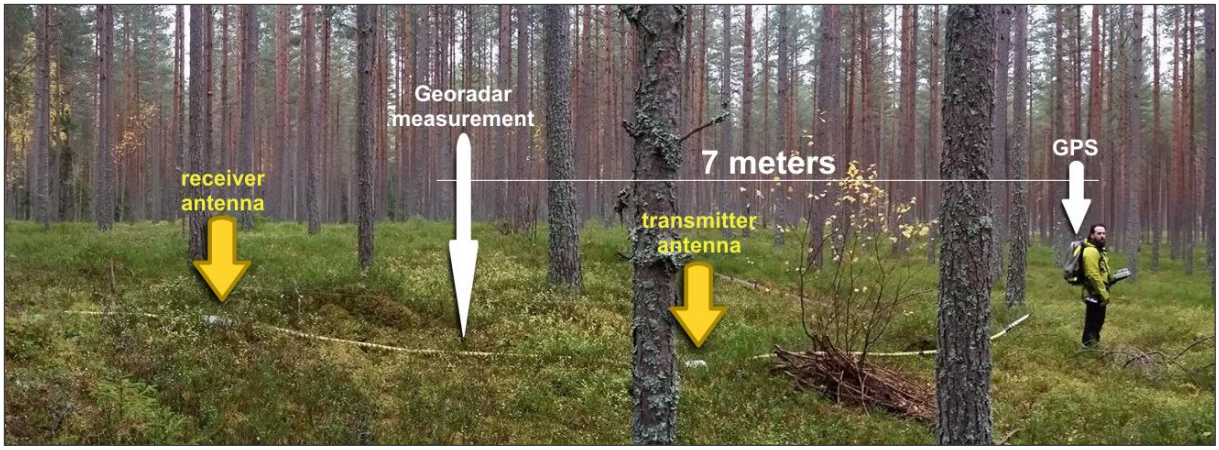

Figure 3.1: Malå Rough Terrain Antenna (RTA) or Snake system deployed in the field with necessary clarifications. Central frequency employed: 100 MHz.

Following the survey, an analysis of the collective Average Trace Amplitude (ATA) plot across all Brumunddal localities indicates that signal attenuation to noise level occurred at a maximum time of 450 nanoseconds, validating the adequacy of the selected time window (Figure 3.2). This analysis also revealed that complete signal absorption was reached between 250 and 550 nanoseconds, corresponding to minimum and maximum depth penetrations of 12.5 and 27.5 meters, respectively.

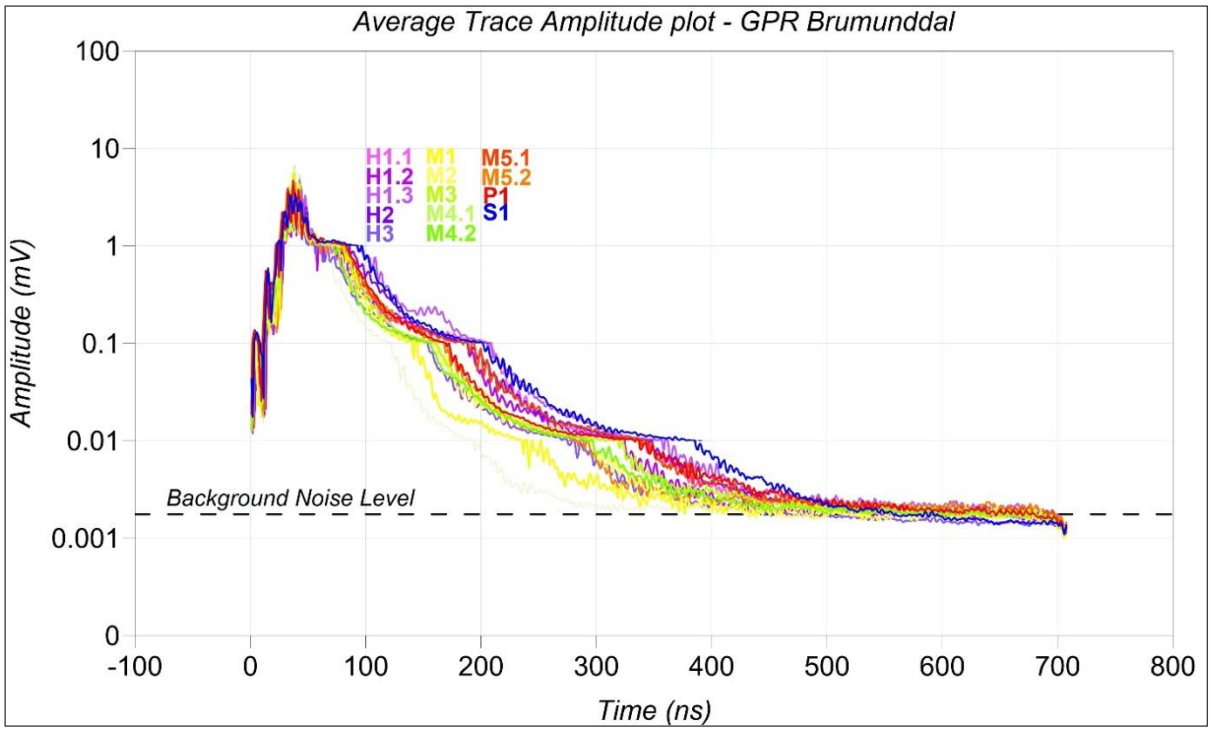

Figure 3.2: GPR signal Average Trace Amplitude (ATA) for the entire Brumunddal survey displaying the minimum and maximum penetration depth achieved.

Figure 3.3 illustrates the location of GPR profiles within the broader Brumunddal area, highlighting the various sediment types surveyed, particularly till of varying thicknesses and peat/bog areas. The literature indicates that till materials exhibit a wide range of electromagnetic (EM) wave velocities, influenced by composition and moisture content (Davis & Annan, 1986; Daniels, 2004).

Wet till typically exhibits velocities ranging from 0.06 to 0.09 m/ns, while dry till can range from 0.09 to 0.12 m/ns.

In this survey, Common Mid-Point (CMP) measurements were not feasible due to the fixed configuration of the Snake system antennas, preventing velocity calibration in the field. Therefore, an average velocity of 0.1 m/ns was chosen for depth conversion, representing a balanced estimate for the till deposits in the area. This assumption allowed for a standardized approach across all profiles and provided a basis for shared interpretations for the whole study area.

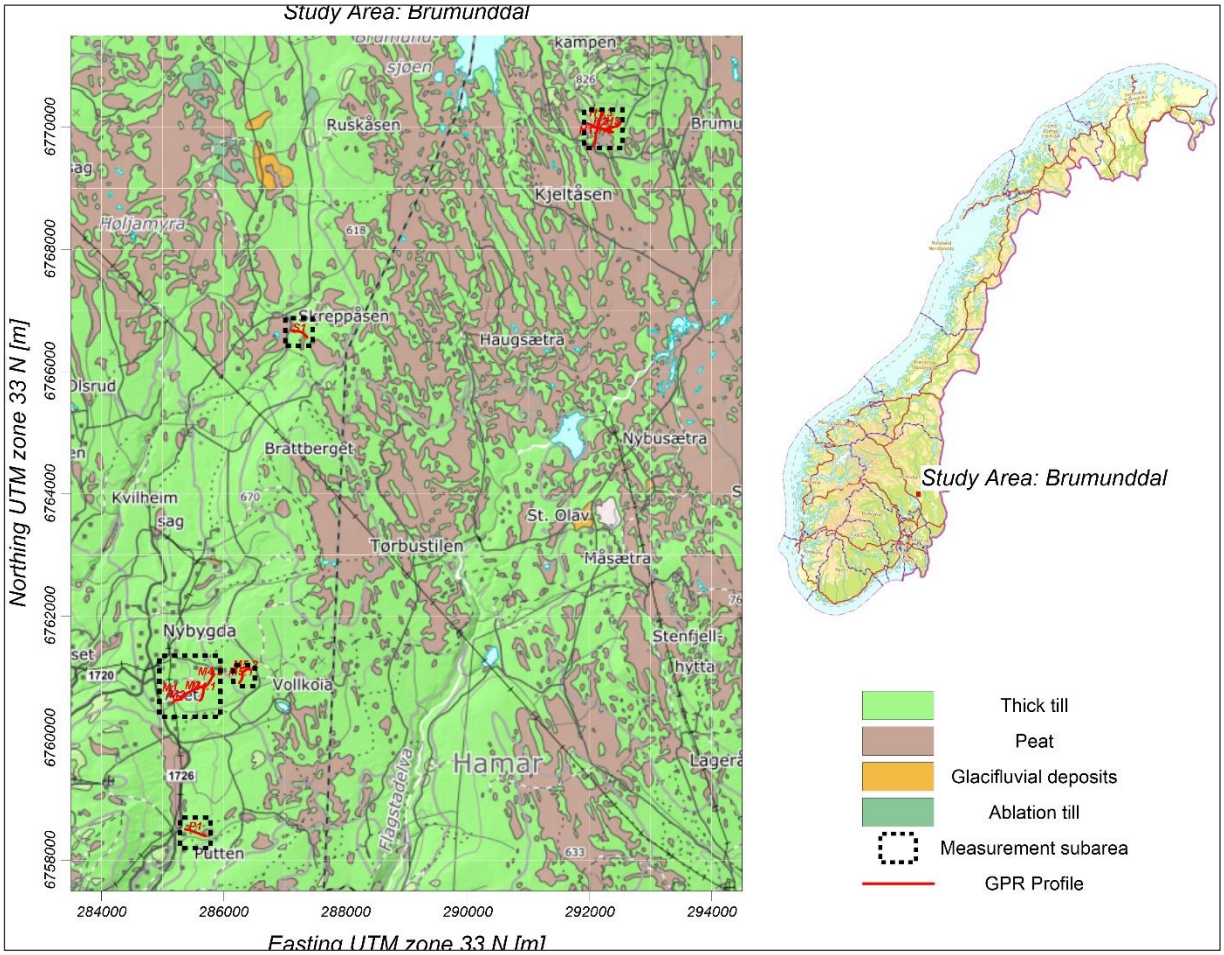

Figure 3.3: Location of the survey area and the GPR profiles measured at Brumunddal, on the Quaternary geology map of the region (Bergstrøm, Sveian, Olsen, & Riiber, 2016).

The preparation of the GPR data involved refining positioning to correct for erroneous points, followed by elevation sampling from available Digital Terrain Models (DTM). In Brumunddal, positioning was recorded using a handheld GPS with a 4-meter error margin. Considering this uncertainty, real-world X-Y coordinates (UTM zone 33 north) were assigned to each trace, complemented by elevation Z values sampled from the Mapping Authority's NDH Brumunddal 5 pkt DTM (Terratec, Laserskanning for Nasjonal Detaljert Høydemodell: NDH Brumunddal 5pkt, 2016). While all data were processed and presented with realistic topographical features, it is important to note that they are not entirely accurate.

All collected data were processed using the software package EKKO_Project v.5 (Sensors & Software, 2018). Initially, data from the Snake system, which were in the rd3 file format, required conversion to the dt1 format to ensure compatibility with EKKO_Project. This conversion was handled by ReflexW v.9.1 software (Sandmeier, 2023). Processing was tailored to each individual profile but remained relatively consistent across the different sites due to similar ground conditions.

Table 1 **Feil! Fant ikke referansekilden.**provides a summarized description of the processing modules used in EKKO_Project v5, offering rounded-up information about each module applied. Overall, the data processing approach was uniform across the surveyed localities.

Table 1: Processing modules employed in EKKO_Project v5.

Processing module	***Value / Description***
Edit First Break	*19 -21 ns*
Bandpass Filter	*Fc1 0 % / Fp1 20 % / Fp2 100 % / Fc2 120 %*
Spatial Median Filter	*Filter Width: 4 pts / Mean: 1 pts*
Migration / Depth conversion	*FK migration: 0.1 m/ns*
Dewow	*Window Width (Pulse Widths): 1.33*
Background Subtraction	*Filter Width: 20 m (rectangular)*
SEC2 Gain	*Attenuation 0.75 – 1.7 dB/m, Start Gain 1.9 – 2.8, Maximum Gain 300 - 700*

4. RESULTS AND INTERPRETATIONS

This section presents and interprets all processed radargrams, organized by subareas within the wider Brumunddal region: Hestbekken, Åsdal, Mælumsætra, Putten, and Skreppåsen. The results from each subarea are presented in maps and by displaying the processed radargrams alongside surface features such as landslide deposits and scars, which are essential for interpretation. All radargrams in this study are presented with their Z-axis (elevation) exaggerated by a factor of two. This vertical exaggeration was applied to make the recorded reflections and stratigraphic details more distinguishable and visually prominent.

Note that the landslide deposits are larger than what is shown on the maps. Only some of the landslide deposits were mapped, recognised by hummocky terrain. Sometimes the deposits were not easy to map due to bog or agricultural levelling.

4.1 Hestbekken

Figure 4.1.1 illustrates the locations of profiles H1, H2, and H3 measured in the Hestbekken area, situated in the northeastern section of the study area (Figure 3.3). Together, these profiles span a total of 1.32 kilometres, traversing a 200 by 250-meter landslide deposit situated centrally within the mapped area. Profile H1, however, is segmented into three parts due to intermittent equipment issues encountered as the profile crossed over bog. These conditions temporarily disrupted the electromagnetic transmission along certain segments of the profile.

The ATA (Average Trace Amplitude) analysis for the Hestbekken GPR profiles reveals that the signal is fully attenuated after approximately 450 nanoseconds, as depicted in Figure 4.1.2. This attenuation time corresponds to a maximum penetration depth of around 22.5 meters, indicating that the subsurface conditions in this area are reasonably favourable for signal propagation. Achieving this depth is notable, particularly given the presence of till and bog, which are typically more challenging environments for GPR due to their variable electromagnetic properties.

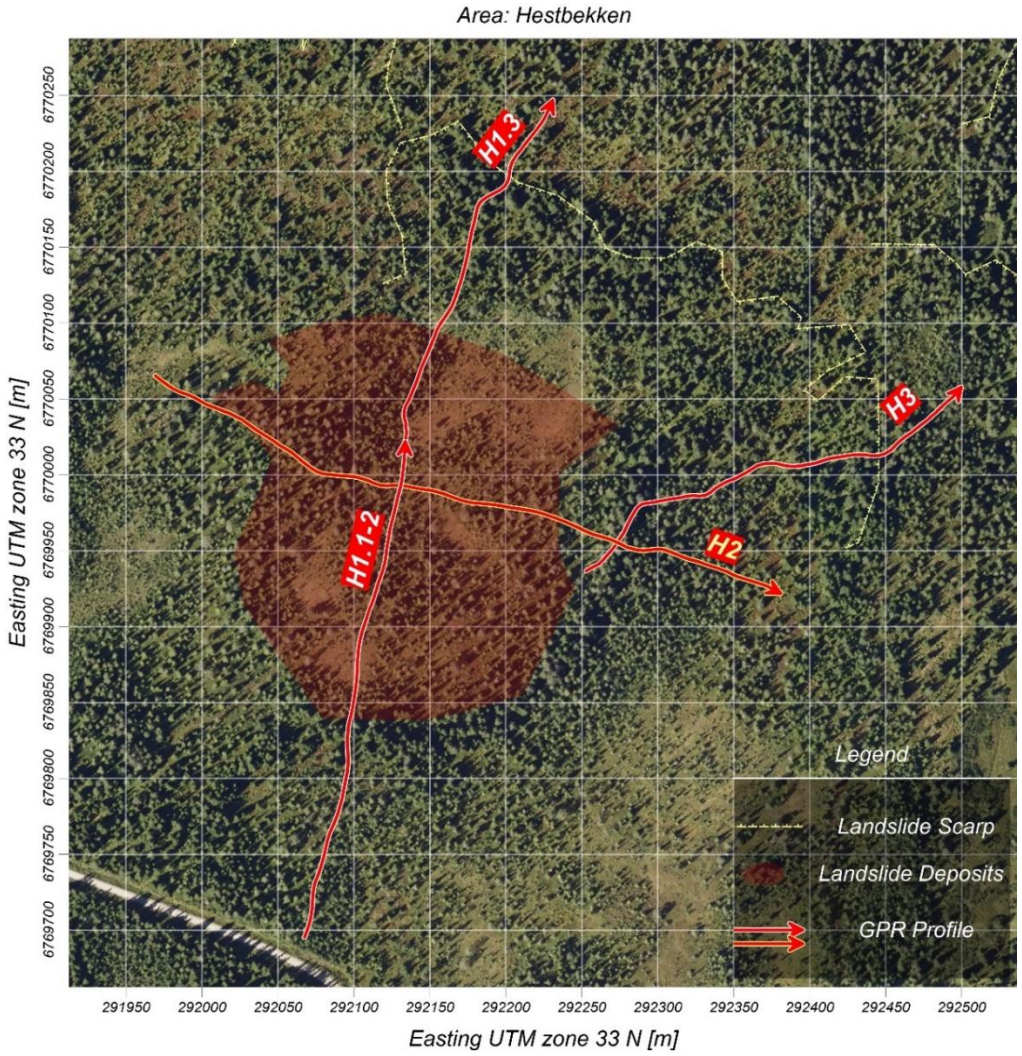

Figure 4.1.1: Positioning of Georadar profiles collected at Hestbekken in relation with landslide scars and some of the landslide deposits mapped in the area. Orthophoto: Østlandet (Terratec, 2016).

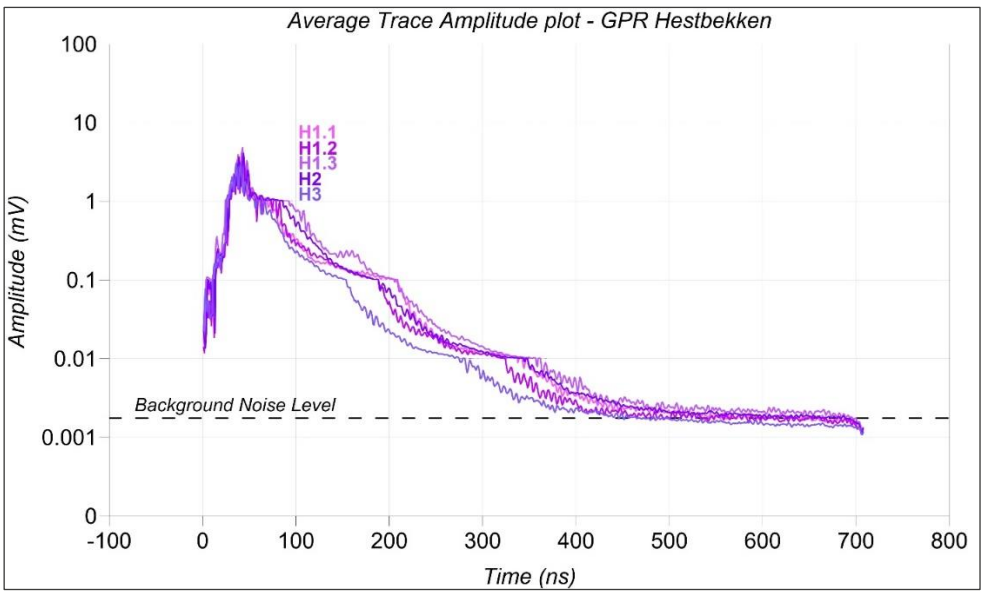

Figure 4.1.2: GPR signal Average Trace Amplitude (ATA) for Hestbekken subarea displaying the penetration depth achieved.

The processing results for GPR profile H1, shown in Figure 4.1.3 (split into two parts for clarity), reveal a complex and somewhat disrupted subsurface structure. The reflections along this profile are generally discontinuous and crisscrossing, with no clear evidence of distinct stratification. This irregular pattern is especially noticeable in the sections beneath the landslide deposits, where the reflections are notably weaker compared to those found upslope, closer to the landslide's backscarp.

One of the most notable findings from these GPR measurements is the results over two separate bog areas our profile traversed. The first bog extends from 140 to 215 meters along the profile (H1.1-2), and the second from 250 meters (H1.1-2) to 110 meters (H1.3). Within these water-saturated zones, no reflections are detected, suggesting a lack of coherent layering within the bogs themselves. However, the GPR successfully maps the bottom of both bogs, revealing a maximum depth of around 5 to 7 meters for each. Beneath the bog, additional strata, likely composed of sediments, are visible extending down to approximately 16-17 meters below the surface.

In the bog at the beginning of profile H1.3, the reflector indicate that the base of the water-saturated zone appears segmented at 55, 75, and 90 meters along the profile, possibly indicating faulting or structural disruption in the subsurface. Finally, the distribution of strong reflections in the profile suggests the presence of sediments, which may indicate that the depth to bedrock is at least as deep as the areas where these strong reflections are observed. This profile provides valuable insight into both the surficial and deeper structures within the landslide and bog areas.

The processed radargrams for profiles H2 and H3, as shown in Figure 4.1.4, indicate slightly varying permittivity conditions across the study area, despite their close proximity with profile H1. With the exception of the initial 100 meters of profile H2 and a few scattered areas, both profiles predominantly display weak reflectivity. This weak reflectivity might suggest either increased water saturation or a shallower bedrock presence, or potentially a combination of both.

Consistent with the observations in profile H1, the GPR has effectively mapped the bottom of the bogs along profiles H2 (between 170 and 280 meters) and H3 (from 40 to 165 meters). However, strong reflections are not registered below these bogs, suggesting a lack of substantial contrast in the materials beneath. While these bog boundaries present the most continuous reflections in the profiles, elsewhere, the reflectors are generally discontinuous, forming local clusters without a lateral pattern of stratification. Additionally, certain reflections beneath the bog and extending south-eastward exhibit a gently undulating character, possibly reflecting minor subsurface variations in sediment composition or structure.

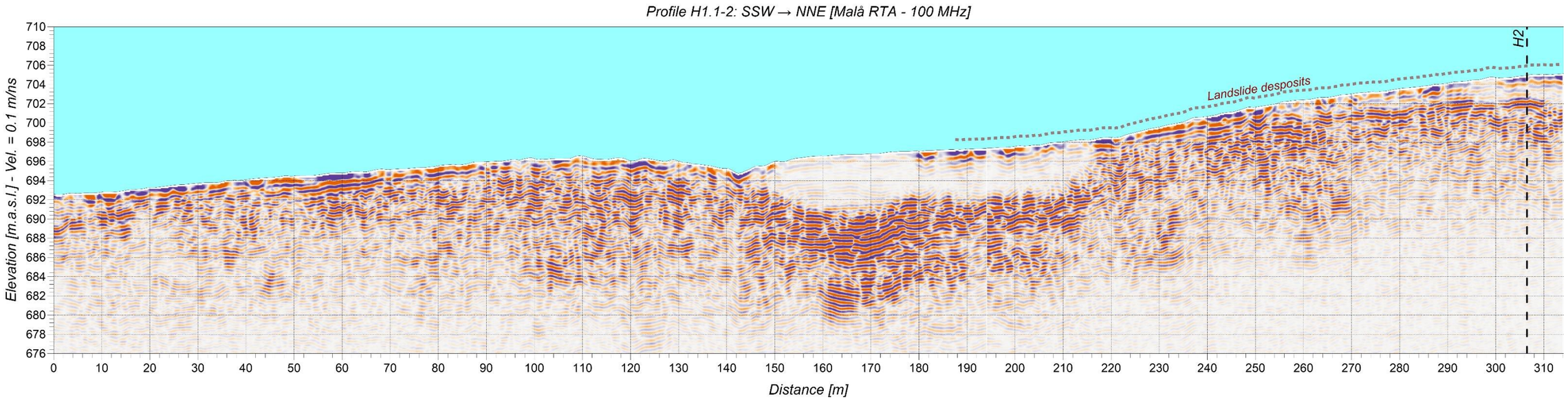

Figure 4.1.3: Processed radargrams for profile H1, showing some of the landslide deposits and scar details.

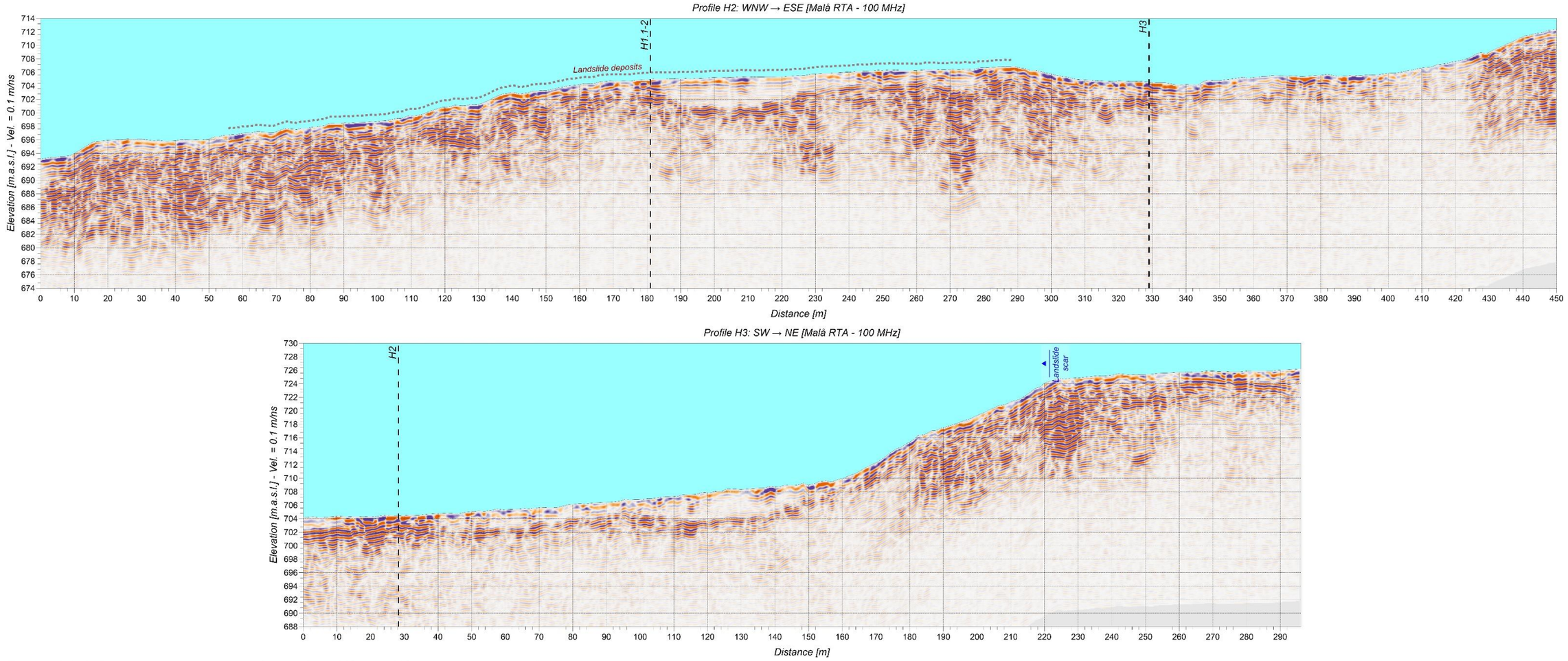

Figure 4.1.4: Processed radargrams for profiles H2 and H3, showing some of the landslide deposits and scar details.

4.2 Mælumsætra – Åsdal

The Mælumsætra subarea, located in the southwest quadrant of the study region, was divided into two parts to manage its size and the extent of the GPR profile coverage. The first part, Åsdal, is displayed in Figure 4.2.1, encompassing four profiles with a total length of 1.26 kilometres. As in Hestbekken, the profiles here are strategically placed to cross a substantial landslide deposition situated on the eastern side of the area. In addition, profile coverage is also extending beyond the landslide boundaries, reaching a landslide scar to the northeast and continuing further southwest. In this region, profiles M3 and M4, due to their longer lengths, are divided into two sections to facilitate clearer presentation and interpretation.

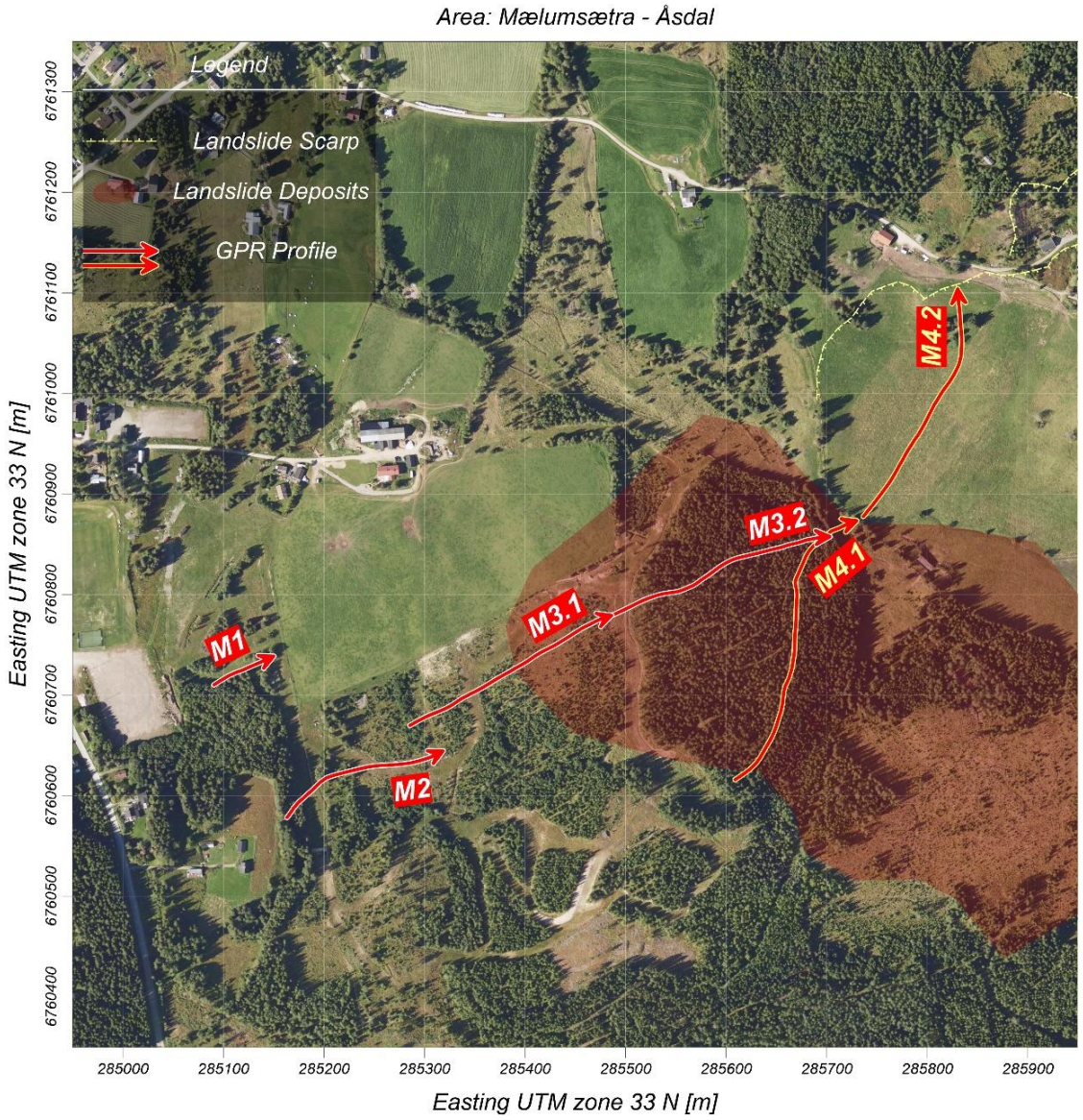

Figure 4.2.1: Positioning of Georadar profiles collected at Åsdal in relation with landslide scars and some of the landslide deposits mapped in the area. Orthophoto: Østlandet (Terratec, 2016).

The ATA plot for Åsdal, as depicted in Figure 4.2.2, reveals a noticeable variation in signal attenuation across the subarea, indicating diverse reflectivity patterns. Profiles M1 and M4.2, west and north of the landslide deposit, display the lowest penetration depths, with the GPR signal attenuating to background noise after 250 to 300 nanoseconds – equivalent to approximately 12.5 to 15 meters of depth. In contrast, profiles situated closer to or directly within the landslide deposits

achieve greater penetration, reaching up to 450 nanoseconds, or about 22.5 meters deep. This variation in signal penetration depth likely reflects different electromagnetic (EM) conditions within the subarea.

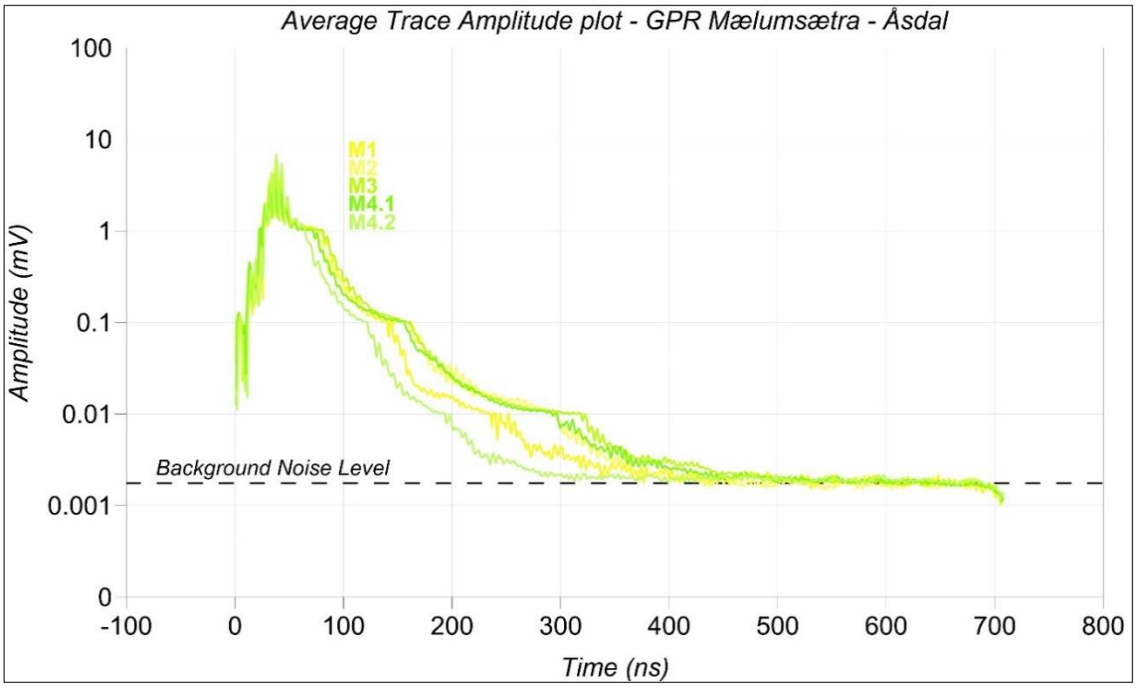

Figure 4.2.2: GPR signal Average Trace Amplitude (ATA) for Åsdal subarea displaying the penetration depth achieved.

Figure 4.2.3 presents the processed radargrams for profiles M1, M2, and M3 (the latter split into two parts), along with the positioning of landslide deposits in relation to the traversing profiles. A clear correlation between the landslide deposits and strong reflectivity is evident in the results. Specifically, the segments of profile M3 located on the mapped landslide deposits display packages of strong reflections that are approximately 10 to 12 meters thick. These reflections exhibit a mildly undulating pattern but are generally discontinuous, indicating variability in the internal structure of the landslide deposits.

Similar patterns of strong reflectivity are observed at the northeastern end of profile M1 and the middle section of profile M2. However, it remains uncertain whether these reflections are also indicative of landslide deposits or represent local concentrations of sand and gravel. Conversely, areas characterized by weak reflectivity may suggest a bedrock hill below the sediments, or sediments less favourable to the transmission of electromagnetic (EM) waves, such as clay or clay-bearing materials.

The processed radargram for profile M4, shown in Figure 4.2.4 split into two sections due to its length, illustrates the contrasting reflectivity patterns in this area. The southern segment, profile M4.1, traverses landslide deposits entirely and demonstrates consistent strong reflectivity down to about 10-12 meters, similar to patterns observed in M3. These reflections show some continuity at depth, particularly around the 446-meter elevation mark, suggesting a more layered structure within the landslide deposits.

In contrast, profile M4.2, which covers farmland and lies outside the landslide deposits, is predominantly marked by weak reflectivity. This segment occasionally features patches of stronger reflections, which could be attributable to localized variations in sediment type or composition. Given the agricultural land cover, this weak reflectivity is likely due to either water-saturated sediments – as farmland may have a higher water content in the surface than other terrains – or remnants of fertilizer. This factor could dampen the electromagnetic signal, diminishing its ability to reveal clear stratification and thus suggesting the presence of sediments rather than bedrock.

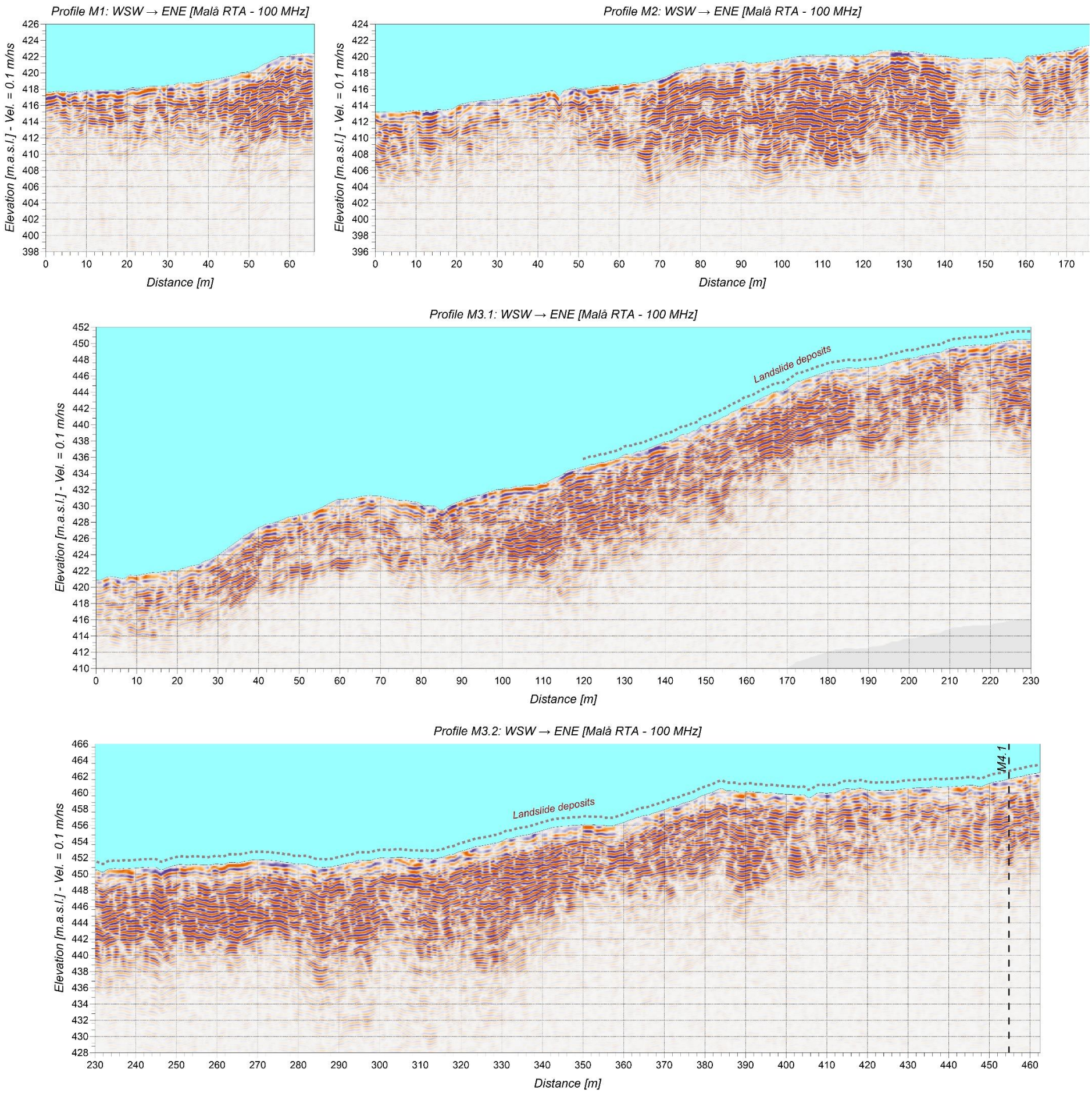

Figure 4.2.3: Processed radargrams for profiles M1, M2 and M3 showing some of the landslide deposits and scar details.

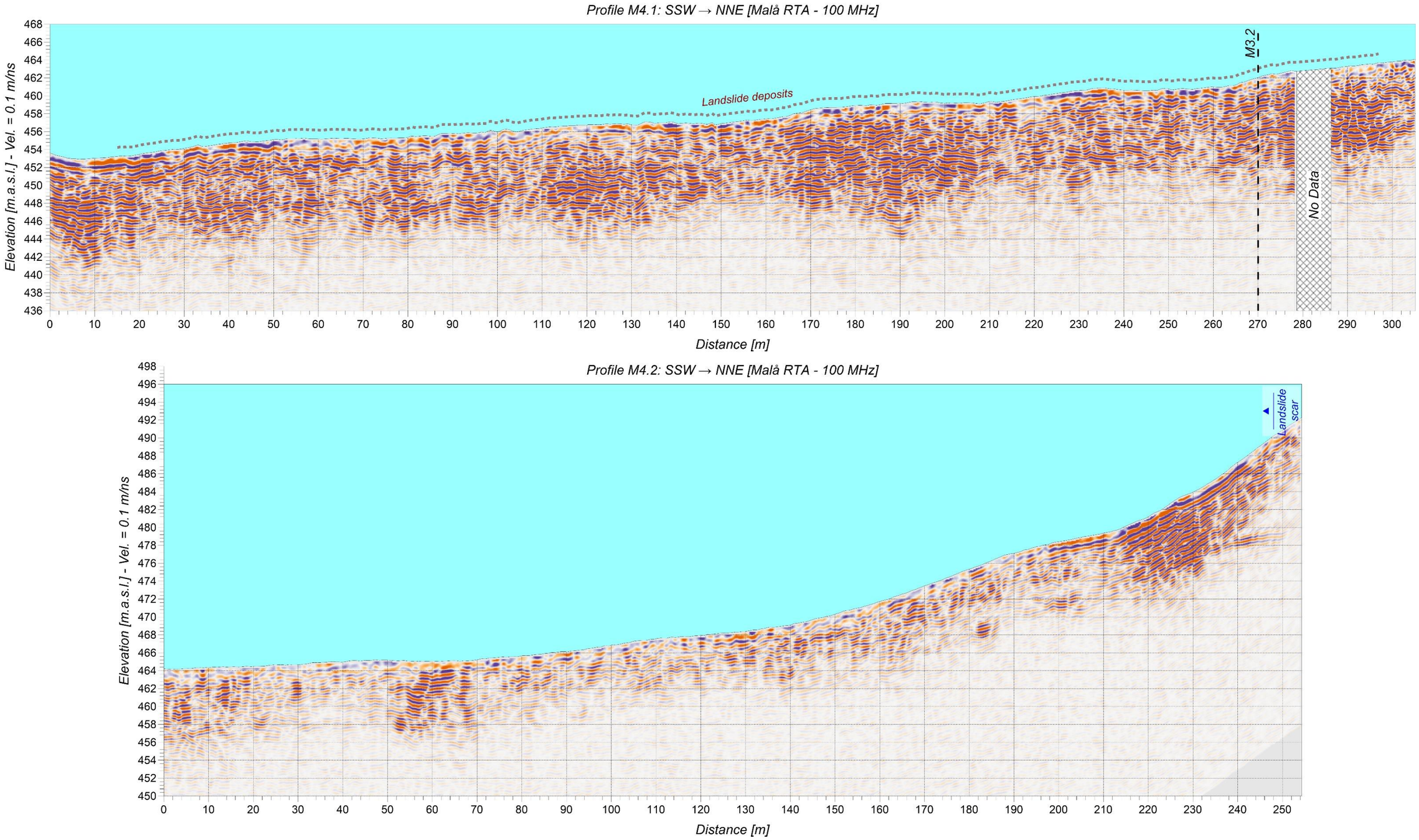

Figure 4.2.4: Processed radargrams for profile M4 showing some of the landslide deposits and scar details.

4.3 Mælumsætra NE

The remaining section of the broader Mælumsætra area, located adjacent to the northeast corner of Åsdal (Figure 3.3), is represented by profile M5. This profile, approximately 320 meters in length, traverses light forest and farmland. Unlike Åsdal, no substantial concentrations of landslide deposits were identified here. However, the area is distinguished by a series of landslide scars, and profile intersects two of them, as illustrated in Figure 4.3.1.

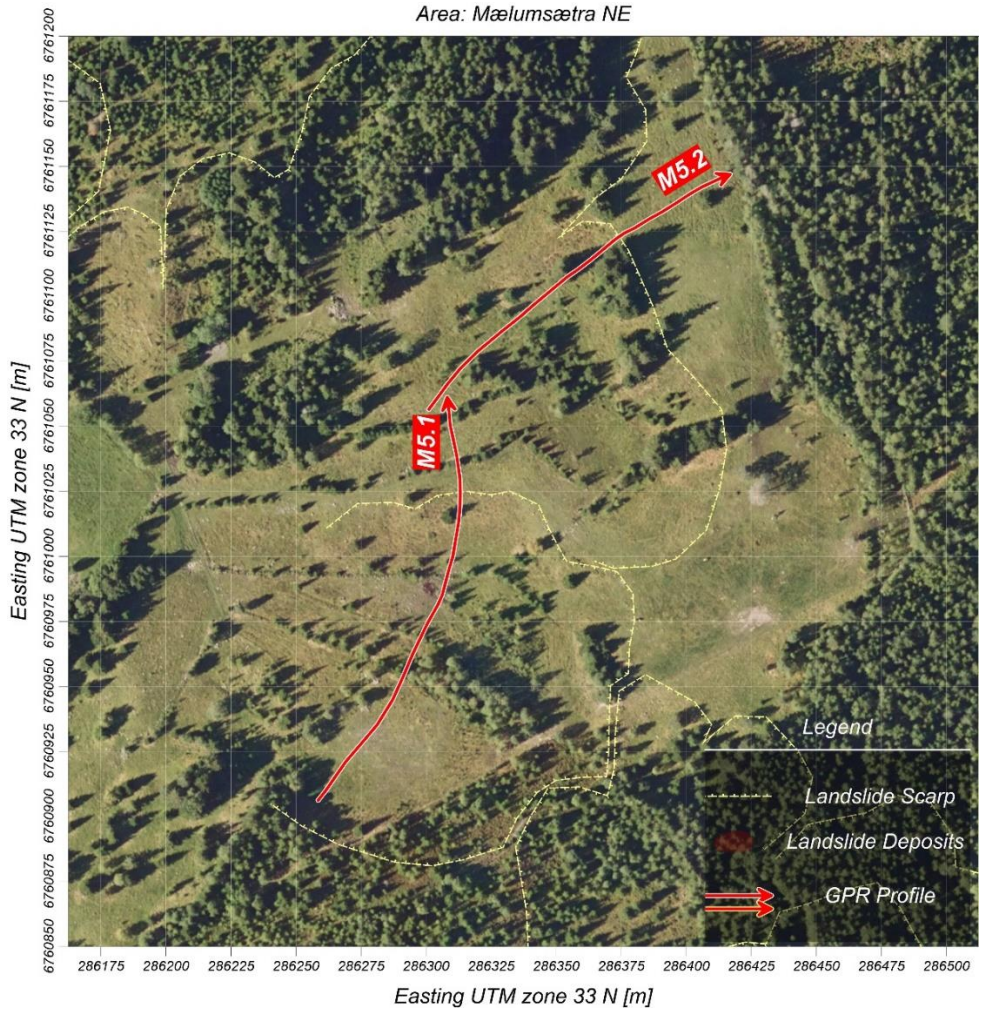

Figure 4.3.1: Positioning of Georadar profiles collected at Mælumsætra NE in relation with landslide scars mapped in the area. Orthophoto: Østlandet (Terratec, 2016).

As shown in Figure 4.3.2, depth penetration in the Mælumsætra NE subarea reaches up to 450 nanoseconds, or approximately 22.5 meters, placing it at the upper limit of the range observed in Åsdal. Notably, the second half of profile M5 (M5.2) experiences slightly faster signal attenuation compared to M5.1. However, this reduction in depth coverage does not significantly impact interpretation, as most of the useful information coming from the use of 100 MHz antennas is generally found within the first 15 meters of depth.

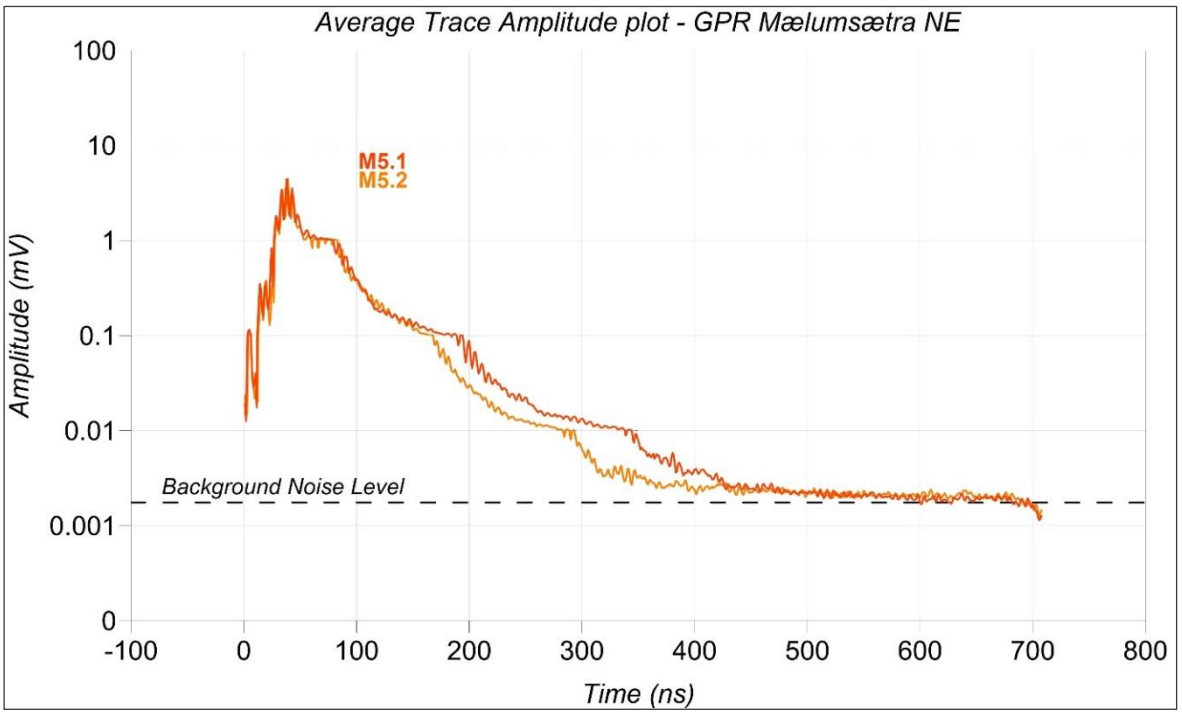

Figure 4.3.2: GPR signal Average Trace Amplitude (ATA) for Mælumsætra NE subarea displaying the penetration depth achieved.

The processed radargrams for profile M5, as seen in Figure 4.3.3, reveal moderately strong reflectivity, particularly along the segment denoted as M5.1. While the reflections here are not as pronounced as those observed in Åsdal, they extend similarly in depth, increasing from approximately 10 meters near the landslide's backscarp to around 16 meters towards the southwestern end of the profile. This suggests a gradual thickening of reflective material with distance from the backscarp. The reflectors exhibit a gently undulating pattern and appear somewhat more continuous than those recorded in other subareas of Brumunddal. This can indicate that even if landslide deposits are not easily mapped on the surface by LiDAR-data, they might be present in the scar bottom. Sometimes the surface is smoothed due to agricultural levelling.

In contrast, segment M5.2 shows pronounced reflectivity as it extends outward from the landslide scar, with reflectivity dropping significantly within the area thought to be directly impacted by past landslide activity. This pattern change is already hinted at the concluding section of segment M5.1, where a strong reflection appears about 5 meters below the surface and closely mirrors the topography along the profile. Beyond this depth, however, few notable reflections are detected, indicating either a lack of distinct layering or the presence of homogeneous material with minimal impedance contrasts. Assuming that landslide deposits are expected to yield strong reflections, we may assume that such materials from the various scars in this area, lie outside the coverage of the GPR profile.

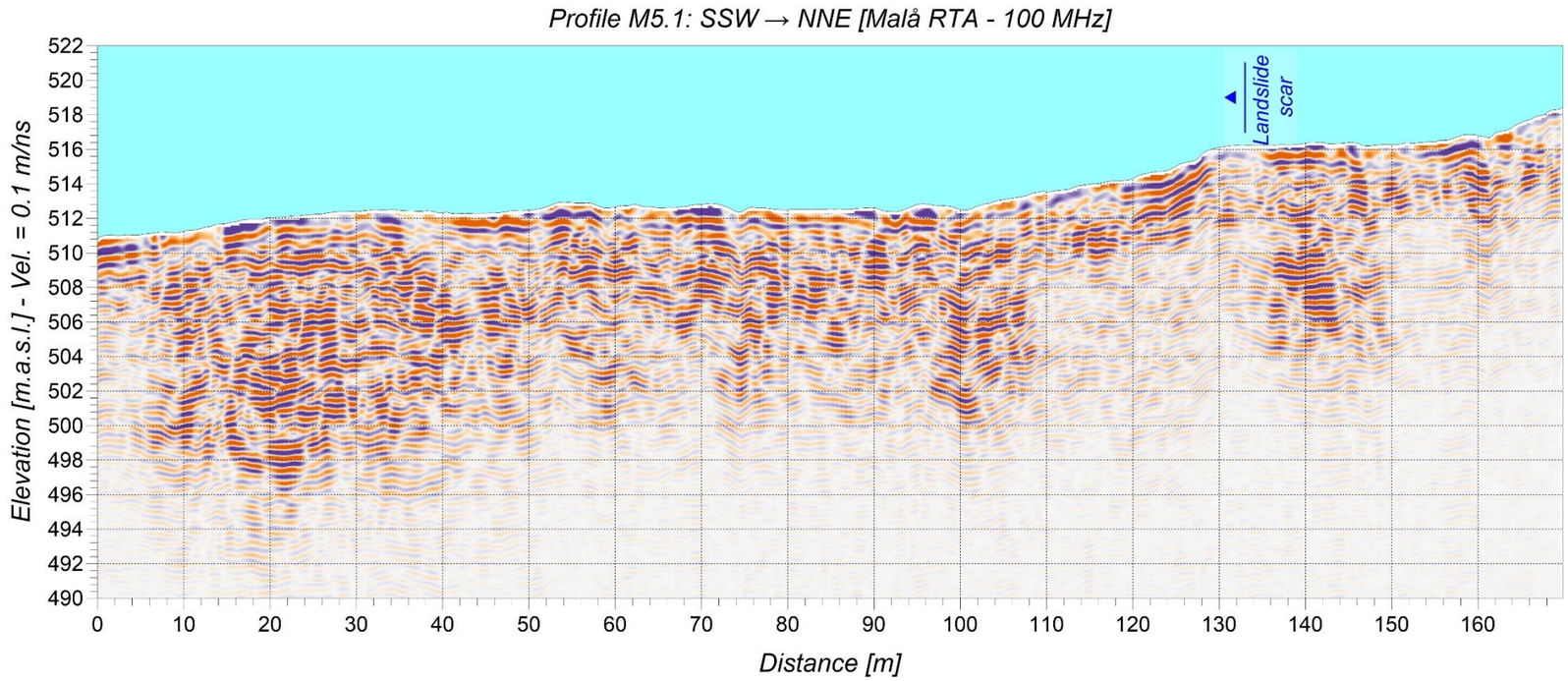

Figure 4.3.3: Processed radargrams for profile M5 showing landslide scar details.

4.4 Putten and Skreppåsen

Putten, located at the southwestern edge of the Brumunddal study area (Figure 3.3), was surveyed using a single 360-meter-long GPR profile, namely P1, depicted in Figure 4.4.1. This profile primarily intersects with landslide deposits, covering almost three-quarters of the northern perimeter of a substantial landslide deposit before moving beyond its boundaries. As shown in the figure, the profile traverses through moderately dense forest and partly in the close-lying scar.

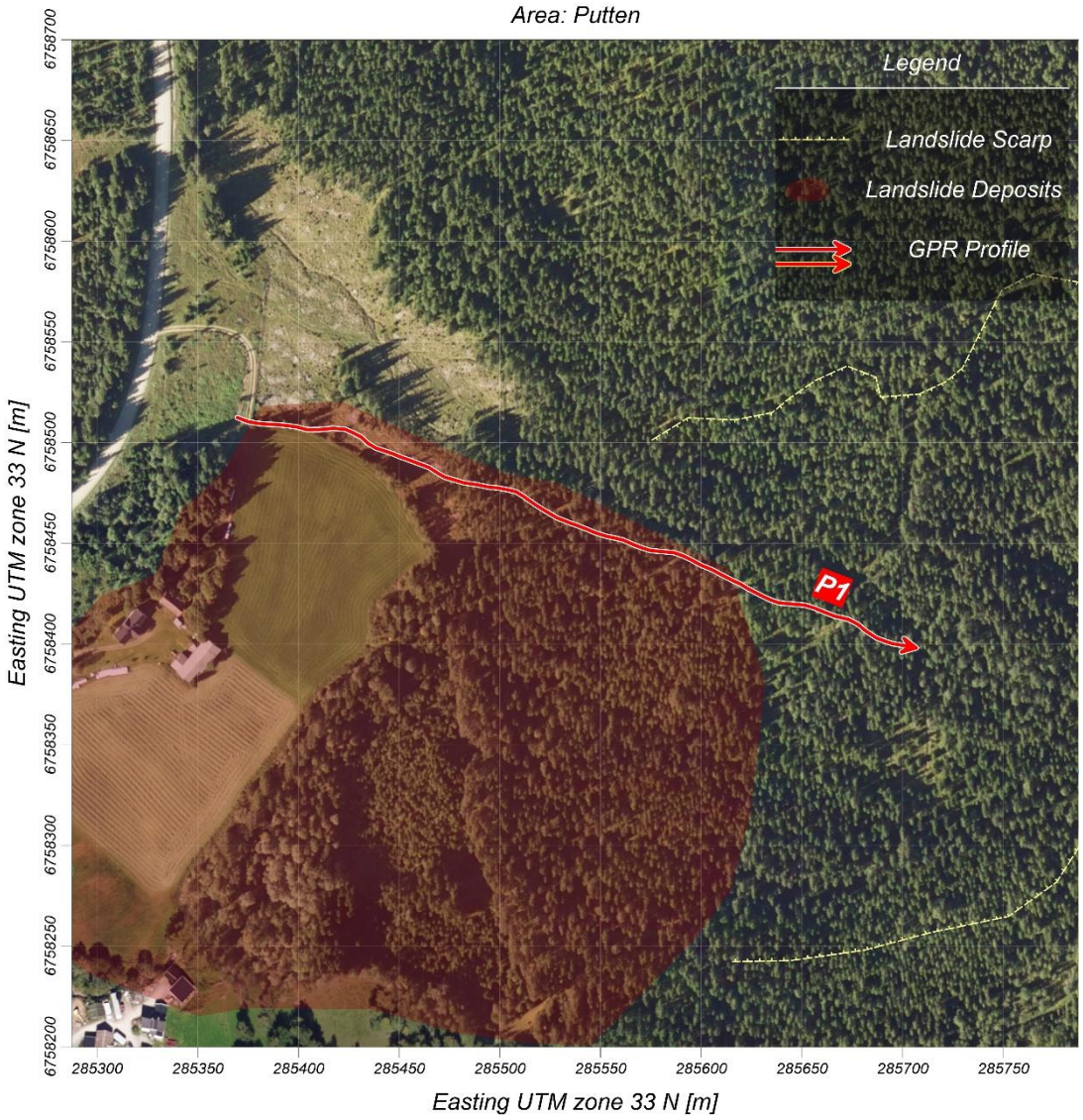

Figure 4.4.1: Positioning of Georadar profiles collected at Putten in relation with the landslide scar and some of the landslide deposits mapped in the area. Orthophoto: Østlandet (Terratec, 2016).

The fifth subarea surveyed in Brumunddal is **Skreppåsen** which lies between Mælumsætra and Hestbekken (Figure 3.3). Figure 4.4.2 shows the measured profile (S1) that extends roughly 300 meters, primarily measured over landslide deposits in moderately dense forest. This profile follows a similar pattern to the Putten survey, intersecting various subsurface features associated with the landslide deposits.

Considering the forested conditions in Putten and Skreppåsen, it is likely that these surveys will likely yield more consistent GPR signal clarity and depth penetration compared to areas with

agricultural land cover. In forested regions, where soil moisture levels are generally lower than in farmland, electromagnetic waves typically experience less attenuation. This results in stronger reflections and deeper penetration depths, facilitating better imaging of subsurface features.

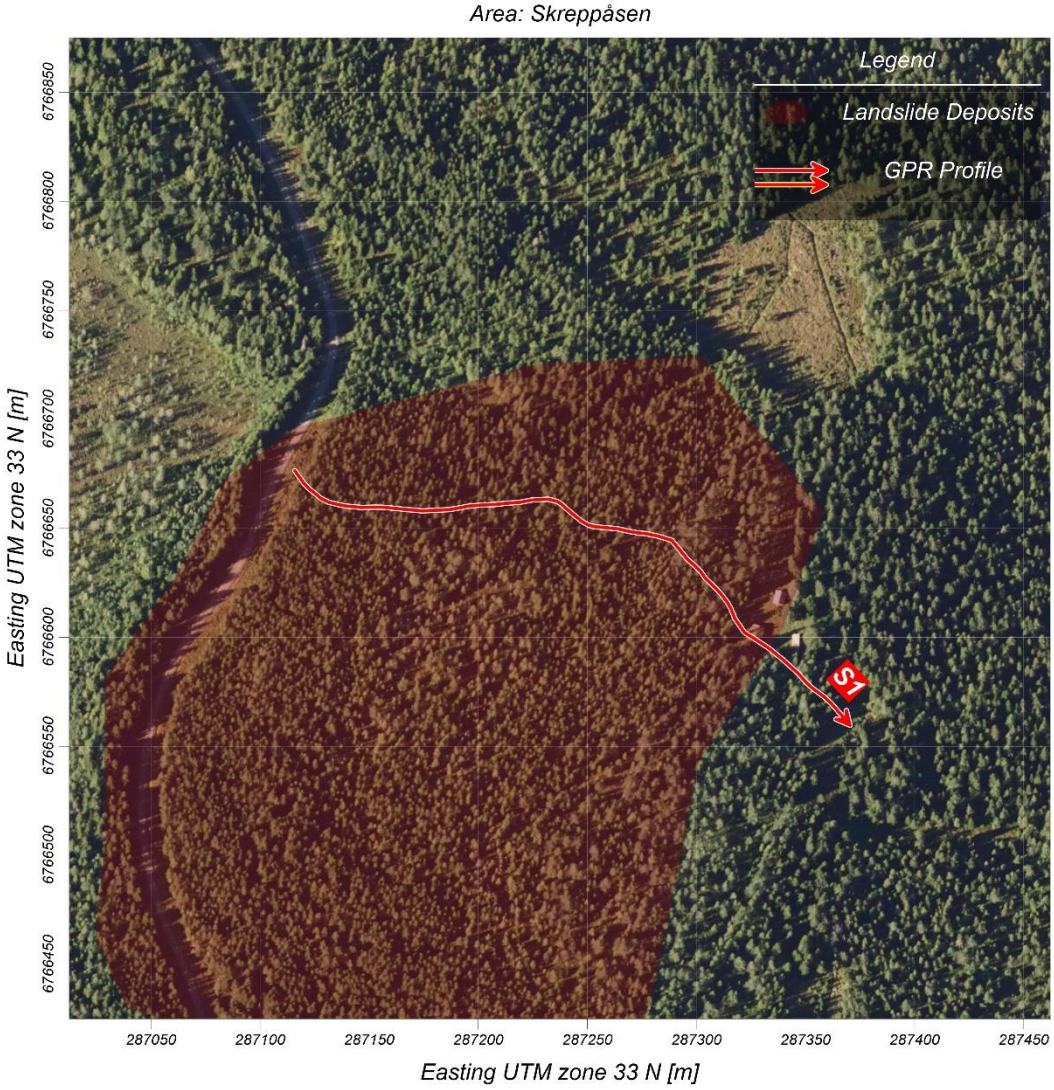

Figure 4.4.2: Positioning of Georadar profiles collected at Skreppåsen in relation with some of the landslide deposits mapped in the area. Orthophoto in background: Østlandet (Terratec, 2016).

The Average Amplitude Plot (ATA) for profiles P1 and S1, shown in Figure 4.4.3, indicates that the GPR signal in these subareas achieved the deepest penetration observed across all surveyed locations within the Brumunddal area. Signal attenuation reaches background noise levels at approximately 550 nanoseconds for both profiles, corresponding to a maximum depth penetration of around 27.5 meters. This depth, however, does not guarantee continuous, clear reflections throughout, as the signal becomes increasingly attenuated and subject to noise as it approaches this limit. The significant penetration depth at Putten and Skreppåsen suggests relatively favourable conditions for electromagnetic wave transmission, possibly due to the specific composition of the subsurface materials or to less saturation or in this area.

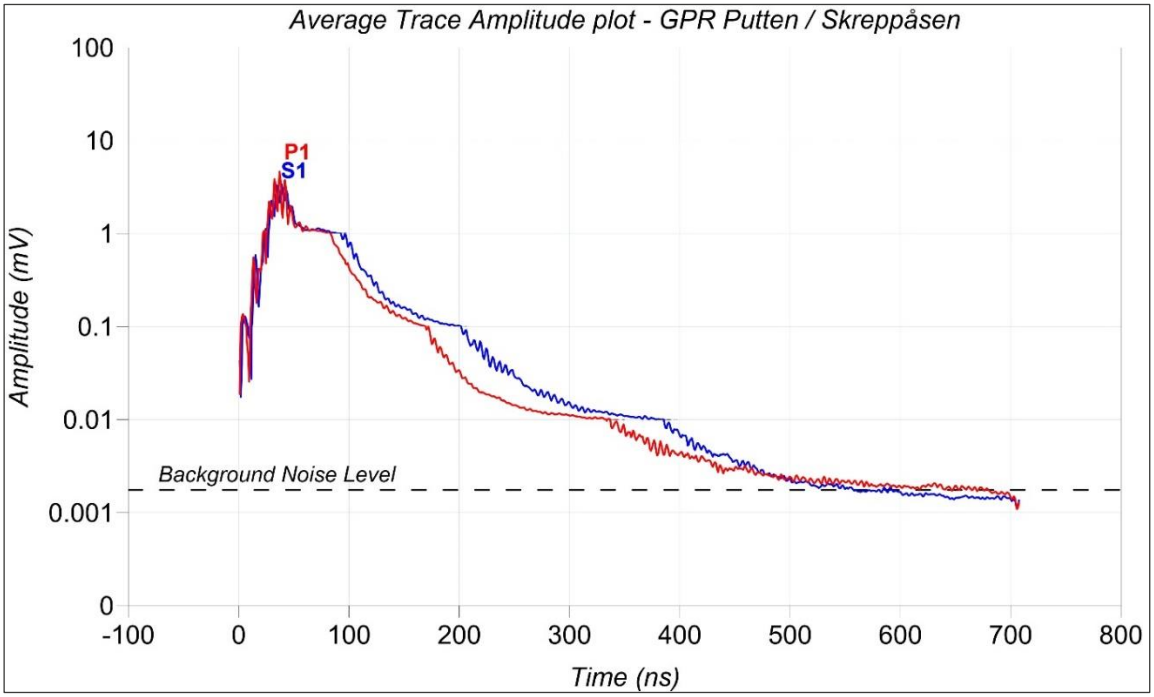

Figure 4.4.3: GPR signal Average Trace Amplitude (ATA) for Putten subarea displaying the penetration depth achieved.

The processed radargrams for profiles P1 and S1, shown in Figure 4.4.4, confirm the advantageous signal conditions suggested by the ATA plot.

Reflectors appear consistently across **profile P1**, with variations in reflectivity thicknesses along the profile's length. Notably, the strongest and thickest reflectors are found inside the landslide scar, reaching up to 17 meters deep. This may be disturbed deposits that was stratified, but not moved out of the scar during the event. Within the mapped landslide deposits, however, reflectivity becomes more irregular. Certain segments, such as those between 50 and 70 meters and between 165 and 190 meters, show strong, continuous reflections, which may indicate the presence of bedrock.

Overall, the reflectors under the landslide deposits appear to have a thickness of roughly 8 to 10 meters, with some local variation. This irregularity could be attributed to differences in material composition, such as variations between landslide deposits and underlying sediments, as well as variations in depth to bedrock and in moisture content and compaction levels across the survey area.

Profile S1, depicted at the bottom of Figure 4.4.4, exhibits a slightly dissimilar distribution of reflectors compared to profile P1. The deepest reflections are notably concentrated in the central part of the profile, specifically between 110 and 150 meters. In this segment, strong reflections extend down to 20 meters below the surface, characterized by relatively sharp lateral edges. This pattern suggests the possibility of a fault zone approximately 40 meters wide or a depression in the topography that existed before the landslide, subsequently filled with sediment deposits.

Outside this central area, the reflectivity of the recorded signals resembles that observed in the Putten area, featuring a shallow zone of roughly 8 meters in thickness where reflectivity is weak. Similar to Putten, this suggests that the underlying materials may consist of less conducive sediment types or conditions, limiting the effective penetration of the GPR signals. The variations in reflectivity across profile S1 highlight the complex subsurface conditions, potentially influenced by geological factors such as faulting or pre-existing topographic features.

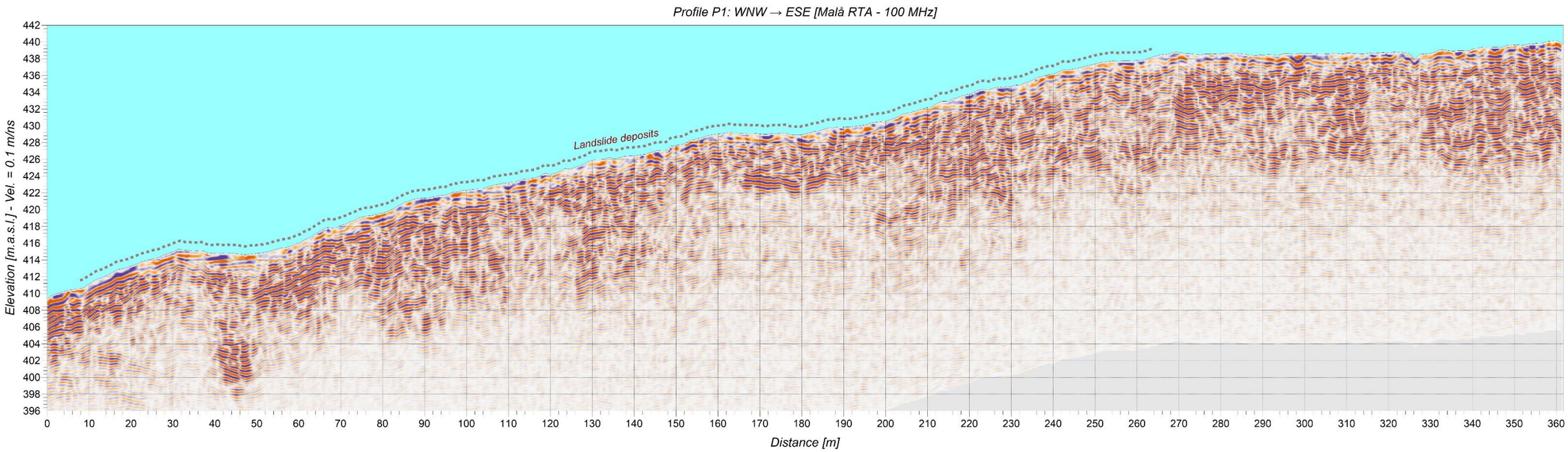

Figure 4.4.4: Processed radargrams for profiles P1 (top) and S1 (bottom) showing some of the landslide deposits and scar details.

5. CONCLUSIONS

This study employed Ground Penetrating Radar (GPR) to investigate subsurface geological features across various localities in the Brumunddal area, focusing on regions affected by post-glacial seismicity and subsequent landslides. The choice of a central frequency of 100 MHz struck a balance between penetration depth and resolution, allowing effective mapping of subsurface features to a maximum depth of approximately 22.5 meters in the subareas Hestbekken, Åsdal, and Mælumsætra NE. In contrast, the Putten and Skreppåsen areas exhibited deeper penetration, reaching up to 27.5 meters. These results highlight the variability of geological conditions encountered, with some profiles indicating more favourable electromagnetic conditions over landslide deposits, characterized by stronger and more continuous reflections.

While a correlation between stronger reflectivity and landslide deposits can be inferred, it is not consistently observed across all measurements. In Hestbekken, Georadar profiles demonstrated both weak and strong reflectivity beneath bogs, suggesting varying degrees of water saturation. Similarly, although profiles in the Åsdal subarea showed correlations between strong reflectivity and landslide materials – confirming that such deposits enhance signal transmission – the presence of distinct reflectors in Mælumsætra was not always consistently linked to known landslide features. We propose that strong reflectivity in areas lacking mapped superficial landslide deposits may represent bog growth or agricultural influence (levelling).

The investigations in the Putten and Skreppåsen subareas further emphasized the impact of surface conditions on GPR measurements. In particular, profile S1 revealed potential faulting or depressions in the subsurface topography, highlighting the complex geological environment of the region. Overall, these findings underscore the necessity of considering local geological and hydrological factors when interpreting GPR data, as they significantly influence the clarity and depth of subsurface imaging.

In conclusion, the GPR survey across the Brumunddal area successfully identified and characterized various geological features, providing valuable insights into subsurface conditions influenced by landslide activity and material properties. Ground truth derived from drilling or excavating these features could further enhance understanding of the factors driving reflectivity in the area and what can or cannot be correlated with landslide activity.

6. REFERENCES

Benedetto, A., & Benedetto, F. (2014). Application Field–Specific Synthesizing of Sensing Technology: Civil Engineering Application of Ground-Penetrating Radar Sensing Technology. In *Comprehensive Materials Processing.* Elsevier.

Bergstrøm, B., Sveian, H., Olsen, L., & Riiber, K. (2016). *Hedmark Fylke, kvartærgeologisk kart, M 1:300 000.* Trondheim: Norges Geologiske Undersøkelse.

Burki, V., Larsen, E., Fredin, O., & Margreth, A. (2009). The formation of sawtooth moraine ridges in Bødalen, western Norway. *Geomorphology Volume 105, Issues 3-4*, 182-192.

Butler, D. (2005). *Near Surface Geophysics (Investigations in Geophysics No. 13).* Society of Exploration Geophysics (First Edition).

Daniels, D. (2004). *Ground Penetrating Radar (2nd Edition).* The Institution of Engineering and Technology.

Davis, J., & Annan, A. (1986). *Borehole radar sounding in CR-6, CR-7 and CR-8 at Chalk River, Ontario: Technical Record TR-401.* Atomic Energy of Canada Ltd.

Fredin, O., Solberg, I., Keiding, M., & Tassis, G. a. (in prep.). Evidence for paleoseismicity in Southern Norway, based on LiDAR-mapping of landslide scars.

Helle, S. (2004). Sequence stratigraphy in a marine moraine at the head of Hardangerfjorden, western Norway: evidence for a high-frequency relative sea-level cycle. *Sedimentary Geology, Volume 164, Issues 3–4*, 251-281.

Lecomte, I., Thollet, I., Juliussen, H., & Hamran, S. (2008). Using geophysics on a terminal moraine damming a glacial lake: the Flatbre debris flow case,Western Norway. *Advances in Geosciences, 14*, 301-307.

Olsen, L., Bergstrøm, B., Sveian, H., & Riiber, K. (2018). *Beskrivelse til kvartærgeologisk kart over Hedmark fylke i M 1:300 000.* NGU Rapport 2017.042.

Sandmeier, K. (2023). *REFLEXW 32 and 64 bit Version 10.3*. Karlsrhue, Germany: Sandmeier Geophysical Research.

Sensors, & Software. (2018). EKKO_Project User's Guide. Mississauga, Canada: Sensors & Software Inc.

Tassis, G., & Rønning, J. (2015). *Comparison between Sensors & Software and Malå GPR equipment based on test measurements at Eikesdalen, Nesset municipality, Norway.* Trondheim: NGU report 2015.046.

Terratec. (2016). *Laserskanning for Nasjonal Detaljert Høydemodell: NDH Brumunddal 5pkt.* Kartverket.

Terratec. (2016). *Rapport for Fremstilling av Ortofoto - Bildedekning: 14231 Omløpsfotografering Østlandet, GSD 25 cm.* Norge i Bilder.

GEOLOGICAL
SURVEY OF
NORWAY

· NGU ·

Geological Survey of Norway
PO Box 6315, Sluppen
N-7491 Trondheim, Norway

Visitor address
Leiv Eirikssons vei 39
7040 Trondheim

Tel (+ 47) 73 90 40 00
E-mail ngu@ngu.no
Web www.ngu.no/en-gb/